# Electron Microscopy and Catalytic Study of Silver Catalysts: Structure Sensitivity of the Hydrogenation of Crotonaldehyde

**Peter Claus*,† and Herbert Hofmeister‡**

*Department of Catalysis, Institute for Applied Chemistry, Rudower Chaussee 5, D-12484 Berlin, Germany, and Max Planck Institute of Microstructure Physics, Weinberg 2, D-06120 Halle, Germany*

*Received: September 24, 1998; In Final Form: January 2, 1999*

Conventional (CTEM) and high-resolution transmission electron microscopy (HRTEM) of $Ag/SiO_2$ and $Ag/TiO_2$ catalysts were combined with reaction studies of the hydrogenation of crotonaldehyde to examine the influence of the silver particle size on activity and selectivity toward the unsaturated alcohol. Nanostructural features of the catalysts, as their silver particle size distribution, mean particle size, and dispersion were markedly dependent on the preparation method. For silica-supported Ag catalysts the selectivity to the unsaturated alcohol was found to be (59 ± 3)%, independent of the particle size in the range of 3.7 nm ≤ $\bar{d}_{Ag}$ ≤ 6.3 nm. Moreover, the specific activities were similar in magnitude and exhibit no clear trend with particle size. Consequently, the hydrogenation of crotonaldehyde over these $Ag/SiO_2$ catalysts appears to be structure-insensitive. Titania-supported silver catalysts reduced in hydrogen at low temperature (473 K, LTR) or high temperature (773 K, HTR), however, showed a quite different behavior. These silver particles exhibit rather narrow size distributions and very low mean particle sizes ($\bar{d}_{Ag}$ = 2.8 ± 1.9 nm for $Ag/TiO_2$-LTR, $\bar{d}_{Ag}$ = 1.4 ± 0.5 nm for $Ag/TiO_2$-HTR), i.e., an exceedingly high dispersion ($D_{Ag}$ = 0.46 and 0.69, respectively). The LTR catalyst gave a higher selectivity to crotyl alcohol (53%) than the ultradispersed HTR catalyst (28%). This pronounced change in selectivity suggests the hydrogenation of crotonaldehyde over these Ag catalysts to be qualified as structure-sensitive with the rate-determining step depending critically on the silver particle size and thus on the silver surface structure. If hydrogenation of the C═O group of the α,β-unsaturated aldehyde is favored by face atoms, most likely the increased fraction of Ag(111) planes of the larger silver particles will give higher formation rates of the desired unsaturated alcohol.

## 1. Introduction

Unsaturated alcohols are important intermediates in the field of fine chemicals synthesis, but the rational design of heterogeneous catalysts applied to the preferred hydrogenation of the C═O group of α,β-unsaturated aldehydes (like crotonaldehyde; see Scheme 1) is not well understood and, thus, has been attracting much interest for fundamental research in catalysis. The selective hydrogenation of α,β-unsaturated aldehydes to produce unsaturated alcohols is much more difficult to achieve than the hydrogenation yielding saturated aldehydes or saturated alcohols because of two reasons: (1) thermodynamics favors hydrogenation of the C═C over the C═O group by about 35 kJ $mol^{-1}$ and (2) for kinetic reasons the reactivity of the C═C group in hydrogenations is higher than the reactivity of the C═O group. Most of the catalysts are based on supported group VIII metals, and various factors controlling the intramolecular selectivity were studied. An increase of selectivity toward unsaturated alcohol can be obtained by the nature of the individual metal,[1,2] by the presence of a second metal in ex situ prepared bimetallic catalysts[3−13] and from metal salt additives in liquid-phase hydrogenations,[14−19] electron-donating ligand effects by supports such as basic zeolites[20,21] and graphite acting as macroligand for platinum and ruthenium particles,[22,23] steric constraints in the metal environment,[20,24−28] strong metal−support interactions (SMSI),[29−37] selective poisoning,[38−40] substitutents on the C═C bond,[7,12,41] and solvent[42−45] and pressure effects.[3,46]

**SCHEME 1**

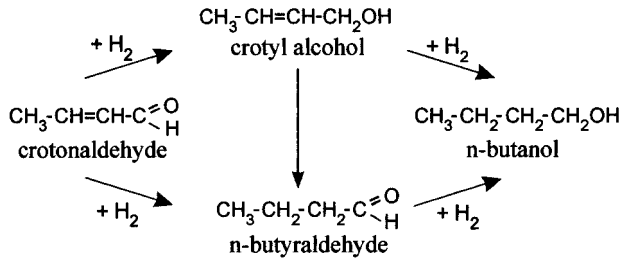


Although among these parameters controlling the intramolecular selectivity the effect of modifying the parent catalyst with a second metal of electropositive character or with oxidized metal species has been widely investigated, the influence of steric constraints on the metal surface, i.e., of particle size effects on selectivity, has been payed less attention and gave, in the case of aliphatic α,β-unsaturated aldehydes, controversial results. Nitta et al. reported that $Co/SiO_2$ prepared by a precipitation method from cobalt chloride exhibits high selectivity to unsaturated alcohols, which increases with increasing mean size of cobalt crystallites.[47−49] The residual chloride in the catalyst precursor was concluded to be responsible for the homogeneous crystallite distribution during reduction in hydrogen. Studies on competitive adsorption between the products of the first hydrogenation step showed a lower adsorption constant on larger

* Corresponding author. Telephone: (+49-30) 6392 4322. Fax: (+49-30-6392 4350). E-mail: claus@aca-berlin.de.
† Institute for Applied Chemistry.
‡ Max Planck Institute of Microstructure Physics.

10.1021/jp983857f CCC: $18.00 
Published on Web 03/19/1999

cobalt particles for the unsaturated alcohol than for the saturated aldehyde.[48] In liquid-phase hydrogenations of higher α,β-unsaturated aldehydes over Pt, Rh, and Ru catalysts, selectivity to the unsaturated alcohol is generally increased with increasing metal particle size.[50−52] On large metal particles, Gallezot et al. claimed that the adsorption of the C═C group of cinnamaldehyde is hindered by a steric repulsion between the metal surface and the aromatic ring, thus favoring hydrogenation of the C═O group.[22,50,52] In contrast, the hydrogenation of citral into unsaturated alcohols (*E*- and *Z*-isomers geraniol and nerol, respectively) over ruthenium catalysts was independent of the Ru particle size.[53,54]

However, data for particle size effects in gas-phase hydrogenations of lower α,β-unsaturated aldehydes such as acrolein and crotonaldehyde are scarce. Coq et al. reported that the selectivity toward allyl alcohol in acrolein hydrogenation over Ru catalysts (at conversions of <1%) is not structure-sensitive.[55] On the other hand, a marked increase of selectivity toward the unsaturated alcohol with increasing platinum particle size has been observed by Lercher et al. studying the hydrogenation of crotonaldehyde over $Pt/SiO_2$ catalysts.[56] The high fraction of Pt(111) surfaces was concluded to favor the adsorption of the α,β-unsaturated aldehyde via the C═O group. By use of a partially reducible support like $TiO_2$ instead of silica and by cycles of high-temperature reduction (at 773 K), oxidation (at 673 K) and a second reduction step (at 473 K), higher selectivities up to 64% were observed.[56] Recently, it has been shown by extended Hückel calculations[57] and experimental studies of hydrogenation of 3-methylcrotonaldehyde (prenal) at 353 K over well-defined surfaces, Pt (111) and Pt(110), that the adsorption mode of α,β-unsaturated aldehydes depends strongly on the exposed crystal face.[58−60] While on Pt (111) the unsaturated alcohol was formed with a selectivity of 65% at 10% conversion,[59] the main products on Pt(110) were the saturated aldehyde (63%) and alcohol (12%).[60] On a catalytic surface that is closer to real catalyst surfaces than low-index planes, namely, Pt(553), which is made up of a regular arrangement of (111) terraces and (111) monoatomic steps, evidence for the structure sensitivity was obtained leading to a lower selectivity of unsaturated alcohol (50% at 10% conversion) than on the Pt(111) surface.[61] Moreover, the stepped platinum surface gave a higher selectivity toward saturated aldehyde than the flat plane (18% instead of 5%).[58]

Recently, we have found excellent catalytic properties of silver catalysts in the hydrogenation of α,β-unsaturated aldehydes[4,41] despite that supported silver is known to be an important oxidation catalyst. The selectivity to the unsaturated alcohol was entirely different from that of conventional monometallic hydrogenation catalysts comprising group VIII metals on nonreducible supports, which do not produce unsaturated alcohols as the main product in gas-phase hydrogenations.[3,46,62] To understand the unusual hydrogenation properties of silver catalysts and to correlate their catalytic behavior with structural features, application of powerful methods of catalyst characterization is necessary. One of these, electron microscopy, assisted by selected-area electron diffraction, has been frequently used to study particle size contribution, crystal habit, surface structure, and surface composition of supported group VIII metal crystallites.[63,64]

In this paper we report detailed characterization of $Ag/SiO_2$ and $Ag/TiO_2$ catalysts by electron microscopy with the aim of studying the influence of the silver particle size on activity and selectivity of the gas-phase hydrogenation of crotonaldehyde. To our knowledge, this is the first thorough investigation of nanostructural properties of silver catalysts and their influence on activity and selectivity in a hydrogenation reaction. Thus, the present study demonstrates the advantageous application of monometallic dispersed silver catalysts for the preferred hydrogenation of C═O functional groups.

**TABLE 1: Designation of the Silica- and Titania-Supported Silver Catalysts Used in This study**

| catalyst designation | preparation method |
|---|---|
| $Ag/SiO_2$-P | precipitation−deposition |
| $Ag/SiO_2$-I | impregnation |
| $Ag/SiO_2$-SG 1 | sol−gel |
| $Ag/SiO_2$-SG 2 | sol−gel |
| $Ag/SiO_2$-SG 3 | sol−gel |
| $Ag/TiO_2$-LTR | incipient wetness |
| $Ag/TiO_2$-HTR | incipient wetness |

## 2. Experimental Section

**2.1. Catalyst Preparation.** Five types of silica-supported silver catalysts prepared by different techniques (precipitation−deposition, impregnation, sol−gel) were used. Details of the preparation procedures have been given previously.[4] Briefly, impregnation of silica (Aerosil 200, Degussa) with an aqueous solution of $AgNO_3$ (Fluka) was followed by drying (373 K, 12 h), calcination in flowing air (448 K), and reduction in flowing hydrogen at 523 K for 3 h to give the final catalyst (catalyst I, 15.6 wt % Ag, $S_{BET} = 153\ m^2\ g^{-1}$). Another silver catalyst was obtained by precipitation−deposition by first adding a solution of silver nitrate to a suspension of Aerosil 200, heating to 353 K followed by addition of an aqueous solution of sodium hydroxide. The catalyst precursor was dried at 373 K for 8 h and reduced at 623 K for 3 h (catalyst P, 77.4 wt % Ag, $S_{BET} = 22\ m^2\ g^{-1}$). Furthermore, three silver catalysts were prepared via the sol−gel technique by first dissolving tetraethoxy orthosilicate ($Si(OC_2H_5)_4$, Fluka) and $AgNO_3$ in a mixed solvent consisting of ethanol, water, and nitric acid or ammonia to perform hydrolysis and gelation under acidic, neutral, or basic conditions, respectively. Then the resulting homogeneous mixtures were refluxed at 353 K for 30−60 min to give solid, chemically homogeneous xerogels. After aging for 48−72 h at room temperature and drying at 373 K for 20 h the precursors were calcined in air at 673 K (4 h) and reduced in flowing hydrogen (90 mL $min^{-1}$) at 623 K (3 h) to give the sol−gel derived $Ag/SiO_2$ catalysts (SG 1, 17.4 wt % Ag, $S_{BET} = 413\ m^2\ g^{-1}$; SG 2, 12.5 wt % Ag, $S_{BET} = 376\ m^2\ g^{-1}$; SG 3, 12.1 wt % Ag, $S_{BET} = 258\ m^2\ g^{-1}$).

Finally, a titania-supported silver catalyst (metal loading 7 wt % Ag) was prepared by incipient wetness impregnation using $TiO_2$ (P25 from Degussa, phase composition of 65 wt % anatase and 35% rutile)[36] as support material and $AgNO_3$ (Fluka) as metal precursor. After drying at 393 K for 10 h, the catalyst precursor was calcined in flowing air (50 mL $min^{-1}$) at 673 K for 2 h. Subsequently, from the calcined material catalyst $Ag/TiO_2$-LTR was obtained by reduction in flowing hydrogen (50 mL $min^{-1}$) for 3 h at 473 K and catalyst $Ag/TiO_2$-HTR by reduction for 3 h at 773 K.

After the materials in a mixture of $HF/HNO_3$ were dissolved by means of an MDS-2000 microwave unit (CEM), the metal content of the silver catalysts was determined by atomic emission spectroscopy with inductively coupled plasma (AES-ICP, Perkin-Elmer Optima 3000XL). The designations of the silica- and titania-supported silver catalysts used in this study are compiled in Table 1.

**2.2. Catalyst Characterization.** The catalysts were characterized by conventional (CTEM) and high-resolution transmis-

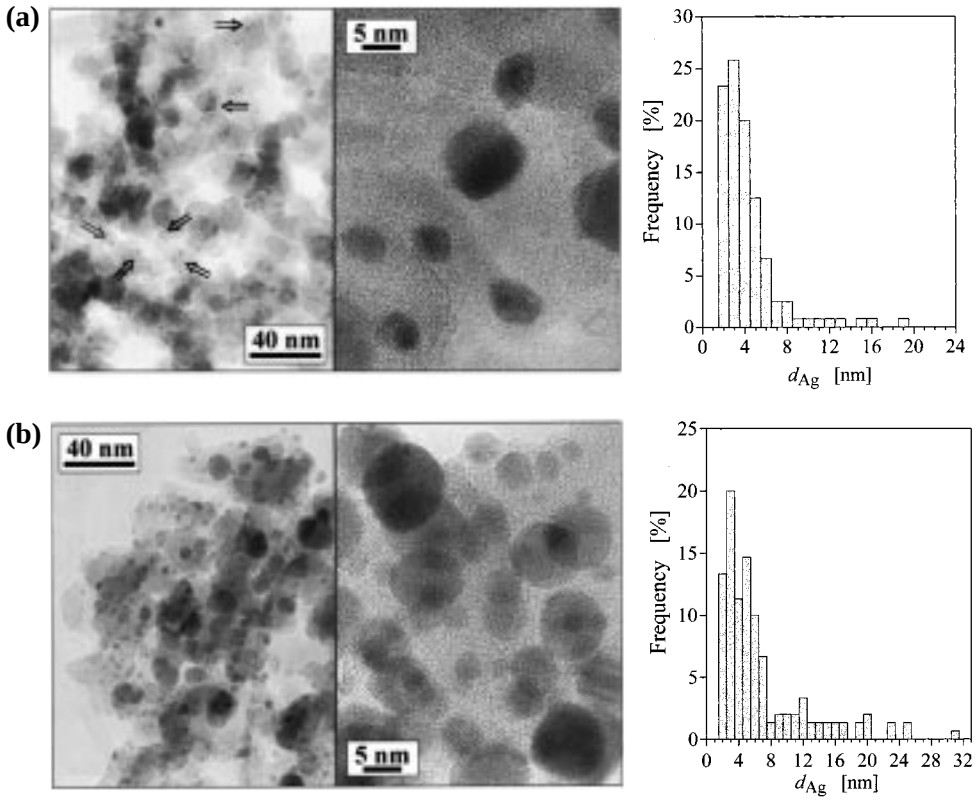


**Figure 1.** CTEM overview with arrows pointing to silver particles (left), HRTEM detailed view (center), and size distribution (right) of catalyst $Ag/SiO_2$-I (a) and of catalyst $Ag/SiO_2$-P (b).

sion electron microscopy (HRTEM). For electron microscopy investigations specimens were prepared by dispersing the catalyst in 2-propanol from which after ultrasonic agitation small quantities were transferred to microgrids coated by thin carbon films. CTEM examination of these specimens was done by means of a JEM 100C operated at 100 kV. Selected area electron diffraction (SAED) was used to confirm crystal structure and crystallinity of the metal loading and, in case of the $TiO_2$ catalysts, also of the support material. A combination of bright-field and dark-field imaging served to distinguish the contrast features of metal particles and finely divided support components to allow evaluation of the size and shape of Ag particles. HRTEM of the specimens was done by means of a JEM 4000EX operated at 400 kV. Micrographs were recorded using optimum imaging conditions (near Scherzer focus) and were subjected to digital image processing for contrast enhancement and image evaluation (software Digtal Micrograph by GATAN and NIH Image[65]).

Catalyst samples were also examined by oxygen pulse chemisorption as described earlier[66] from which the ratio O/Ag at 443 K was determined.

**2.3. Catalytic Hydrogenation of Crotonaldehyde.** Gas-phase hydrogenation of crotonaldehyde (CA, Aldrich, distilled before use) was carried out in a computer-controlled fixed-bed microreactor system, which has been described in detail elsewhere.[67] This equipment allows the performance of high-pressure gas-phase hydrogenations of unsaturated organic compounds that are usually liquids with low vapor pressures under standard conditions (STP). The reactor effluents were on-line-analyzed by an HP 5890 gas chromatograph equipped with a flame ionization detector and a 30 m J&W DB-WAX capillary column. All catalysts were reduced in situ under the conditions described above. The reaction conditions of the crotonaldehyde hydrogenation were the following: temperature range 413 K $\leq T \leq$ 533 K, total pressure $p = 2$ MPa, molar ratio $H_2/CA = 20$, reciprocal space time $W/F = 19$ $g_{cat}$ h $mol^{-1}$ where $W$ is the weight of catalyst (0.23 g; particle size 0.2−0.4 mm) and $F$ is the molar flow of crotonaldehyde. The selectivities of reaction products were calculated from moles of product formed per moles of crotonaldehyde converted, and the steady-state activities of the catalysts were expressed as specific activities (on a gram of catalyst basis) or in the form of turnover-frequencies (TOF).

## 3. Results and Discussion

**3.1. Nanostructural Characterization of $Ag/SiO_2$ Catalysts.** Structural characterization by electron microscopy of real catalysts is generally complicated by strong contrast features originating from the support material by the random orientation of metal particles and by superposition of particle images because of the nonplanar morphology of the catalyst. It is impossible, therefore, to determine all structural features of interest, like size, surface density, shape, and structure of the metal particles, from one single micrograph. Since the figures shown below always give only a selection of such a micrograph, it should be stated that it needs comparison and rating of a considerable number of micrographs in order to extract information from the large number of particles forming the catalyst.

Figure 1 shows a CTEM overview and an HRTEM detail view together with the corresponding size distribution of catalyst I (a) and of catalyst P (b). From this comparison it becomes clear that unambiguous assessment of metal particles may not be based on CTEM bright-field images only but must be complemented by dark-field images (not shown here) and/or HRTEM images. Even if the latter images do not always exhibit lattice plane fringes because of the random particle orientation and contrast deterioration by thick amorphous support components, the considerably higher accelerating voltage used results

**TABLE 2: Results[a] of Catalyst Characterization and Crotonaldehyde Hydrogenation[b] over $Ag/SiO_2$ Catalysts**

| $Ag/SiO_2$ catalyst | $\bar{d}_{Ag} \pm \sigma$[c] [nm], TEM | $D_{Ag}$[d] TEM | O/Ag | activity [$\mu$mol $g_{Ag}^{-1}$ $s^{-1}$] | TOF/$10^{-3}$ [$s^{-1}$][e] | $S_{CyOH}$ [%][f] |
|---|---|---|---|---|---|---|
| P | $6.3 \pm 5.4$ | 0.24 | 0.006 | 4.7 | 1.1 | 58 |
| SG 2 | $4.6 \pm 3.3$ | 0.31 | 0.058 | 8.9 | 1.5 | 63 |
| I | $3.9 \pm 2.9$ | 0.35 | 0.27 | 3.4 | 0.5 | 61 |
| SG 1 | $3.7 \pm 3.4$ | 0.37 | 0.037 | 4.4 | 0.6 | 56 |
| SG 3 | $3.7 \pm 3.3$ | 0.37 | 0.098 | 10.3 | 1.5 | 57 |

[a] Arranged with decreasing silver particle size. [b] Reaction conditions: $T = 413$ K, $p_{total} = 2$ MPa, molar ratio ($H_2$/crotonaldehyde) = 20. [c] Mean value of silver particle diameter $\pm$ standard deviation by TEM analysis. [d] Silver dispersion by TEM analysis. [e] Turnover-frequency based on $D_{Ag}$. [f] Selectivity to crotyl alcohol.

in more clear particle images. The shape of the metal particles of these two, as well as of the other silica-based catalysts, does not vary significantly with the route of synthesis. The vast majority of particles exhibits a nearly spherical shape. Distinct deviations caused by particle coalescence occur mainly at particles that more than twice exceed the mean particle size. As expected, Figure 1 confirms the relatively low surface density of metal particles obtained by impregnation synthesis in comparison to that of the catalyst prepared by precipitation. This comparison does not include particles that are, mainly because of their extremely small size (less than about 1 nm), "invisible" for electron microscopy inspection.

Quantitatively, the catalysts may be compared by particle size distributions yielding the mean particle diameter, $\bar{d}_{Ag}$, together with its standard deviation, $\sigma$ (summarized in Table 2), as the most important parameters. While $\bar{d}_{Ag}$ and $\sigma$ are 6.3 and 5.4 nm for catalyst P (prepared by precipitation−deposition), indicating a broad size distribution, significantly lower values, i.e., 3.9 and 2.9 nm, respectively, are obtained for catalyst I (prepared by impregnation). The corresponding silver dispersion roughly was estimated from the ratio of the number of surface atoms to the total number of atoms calculated for the mean particle size by assuming particles of closed-shell spherical shape. This leads to a dispersion value of 0.24 for catalyst P and of 0.35 for catalyst I. Because of the low frequencies of rather large particles, these values do not substantially change by consideration of the whole size distribution.

As will be demonstrated also for the other catalysts, the particle size distribution, mean particle size, and Ag dispersion are markedly dependent on the preparation method. Figure 2 shows a CTEM overview, an HRTEM detailed view, and the size distribution of the three catalysts prepared via the sol−gel technique. While preparation under acidic as well as basic conditions yields catalysts having a high surface density of Ag particles with narrow size distribution, neutral conditions lead to a somewhat lower surface density and broader particle size distribution. Accordingly, the silver dispersion calculated from the mean particle size amounts to 0.37, 0.37, and 0.31 for the catalysts SG/A, SG/B, and SG/N, respectively. Thus, the measurements clearly reveal that both impregnation and the sol−gel technique gave higher silver dispersion values than precipitation−deposition.

It must be noted here that upon dispersion in 2-propanol and subsequent ultrasonic agitation, a certain share of the metal particles (varying with the route of synthesis) is situated directly on the carbon film of the TEM grid outside the catalyst support material. The extent to which this occurs may be considered as a rough and qualitative measure of the Ag particle/support interaction strength (work of adhesion). Remarkably, it is mainly the small-sized fraction of Ag particles that establishes themselves as "support-free" particles, which is a result of their weak anchoring to the support. This peculiarity allows imaging of the particle structure without interference from a support contrast. As an example, Figure 3 shows a selection of Ag particles of catalyst SG 1 that exhibit typical shape and spatial composition. First, there are present monocrystalline particles of nearly cuboctahedral shape, designated as COP. A second class of particles contains a single twin plane, i.e., a mirror plane in the lattice of the otherwise monocrystalline particle. These are designated as STP. The third class of particles, designated as MTP, is composed of tetrahedral subunits multiply twinned to each other to form particles of decahedral or icosahedral shape.[68] From COP's to STP's and to MTP's the sphericity of the particles increases accompanied by an increase of the portion of (111) type low surface energy faces. This classification of particle shape and spatial composition also is valid for larger particles of nearly spherical shape situated on the actual support material. Exceedingly large particles, however, frequently contain a set of parallel twin lamellae.

An additional phenomenon to be observed more clearly at the "support-free" particles is the covering of metal crystallites by amorphous layers. This was most pronounced for the catalyst SG 3 from which Figure 4 shows an example. The monocrystalline Ag particle of nearly cuboctahedral shape is coated entirely by an amorphous layer forming a shell of irregular shape, with a thickness of about 0.5−1.5 nm. The shell contrast may be clearly distinguished from that of the amorphous carbon film. Since the origin and nature of such shells must remain unclear for the moment—maybe these are carbonaceous layers due to organic impurities from the catalyst synthesis or even remnants of the support material tightly bound to the metal—their blocking effect on the catalytic properties is unambiguous. The occurrence of marked particle coverage may be estimated to be less than one-quarter of the "support-free" particles of catalyst SG 3. A closer investigation of the nature of these layers would require, for example, electron energy loss spectroscopy with high spatial resolution. Similar capping layers have been observed at the titania-supported catalyst, which will be presented below.

Note that other characterization methods such as X-ray diffraction or chemisorption can give an overestimation of the particle size. In particular, this will happen if the prevailing part of the metallic phase consists of a highly dispersed metal, thus invisible to XRD, or if metal particles covered by support material are not accessible to probe molecules of chemisorption.[4,46,69] Table 2 includes the results of oxygen chemisorption from which silver particle sizes can be calculated using the relation $\bar{d}_{Ag} = 1.3/(O/Ag)$.[70] Except for the catalyst I that shows a quite normal chemisorption behavior, the fraction exposed (O/Ag), i.e., the silver dispersion, is about 1 order of magnitude lower than the TEM-derived values. Apparently, there is a whole class of small-sized Ag particles not accessible for the probe molecules of chemisorption. In the case of the sol−gel derived $Ag/SiO_2$ catalysts, it is likely that the silver particles are either surrounded by silica or partially buried within the silica framework, leading to a reduction of the accessible metal surface area. Depending on the route of synthesis, there may be also contributions from covering the metal by residual organic material or even by modification of the electronic properties of metal particles through their coordination to silica.[71] Whereas the latter issue is not considered in this study, the blocking of the particle surface by components of the support material or organic remnants will be further discussed below. The exceedingly low O/Ag value for the catalyst P prepared by precipitation−deposition is of unclear origin. Although not confirmed

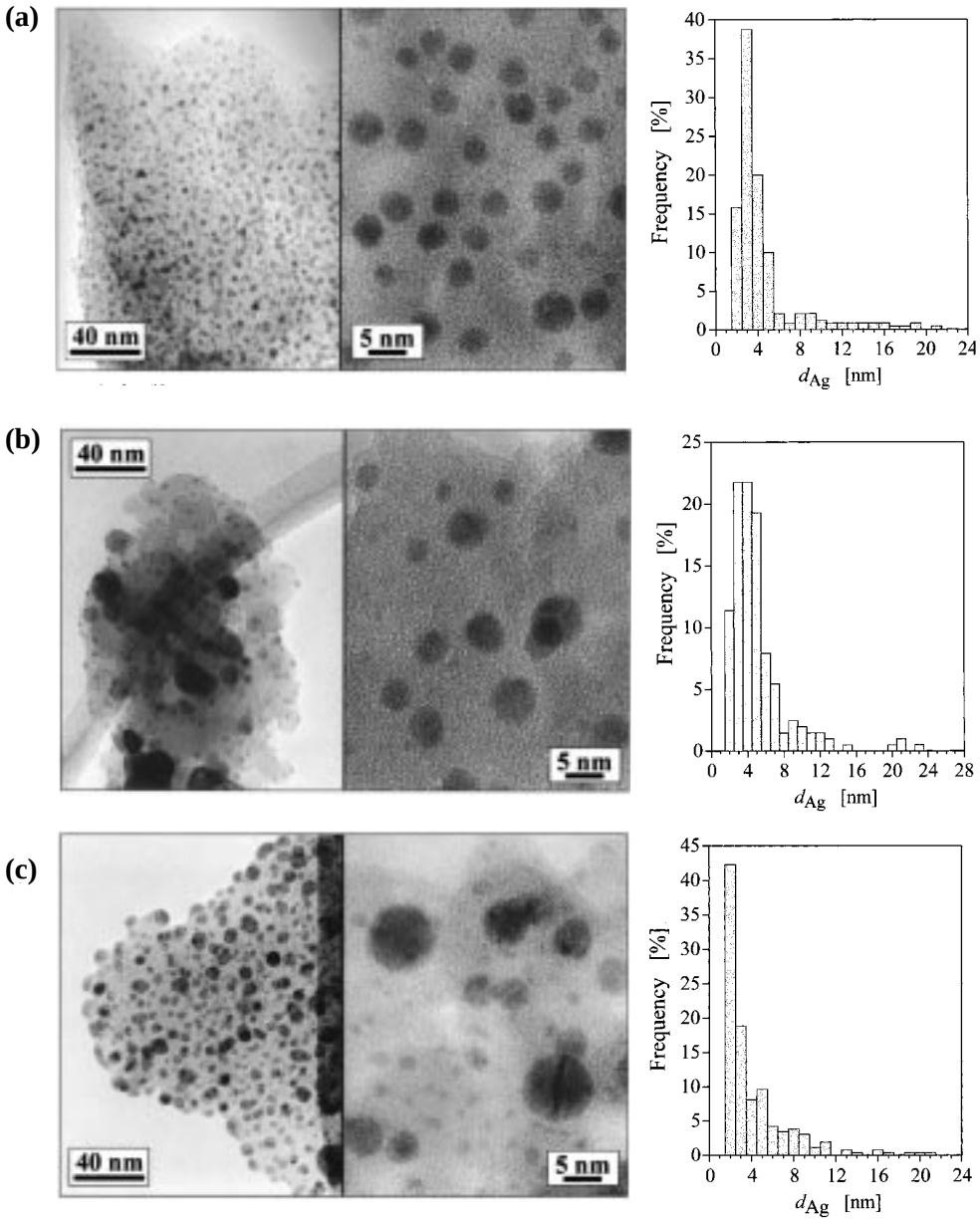


**Figure 2.** CTEM overview (left), HRTEM detailed view (center), and size distribution (right) of the catalysts $Ag/SiO_2$-SG 1 (a), $Ag/SiO_2$-SG 2 (b), and $Ag/SiO_2$-SG 3 (c).

by CTEM or HRTEM because of the almost complete absence of "support-free" particles, we speculate that in addition to the unusually high silver content, presumably residual organic impurities remaining from the preparation prevent suitable $O_2$ uptake[72,73] of the Ag surface. Vannice et al. showed that the choice of the calcination and reduction temperatures had a marked influence on oxygen adsorption capacity with maximum silver surface areas being obtained after a 773 K calcination step followed by a 673 K reduction step.[73] The sensitivity of silver to its environment can give variations in oxygen adsorption with silver catalyst pretreatment due to surface reconstruction and crystallite redispersion or changes in the surface composition and formation of subsurface oxygen. Note that our Ag catalysts were catalytically tested after calcination and reduction, under conditions described in the experimental part but without any special pretreatments as usual for oxygen adsorption studies. Dispersions and thus turnover frequency data, based on dedicated model adsorption studies, would be rather unreliable. Therefore, in this study, we calculated TOF data from TEM-derived Ag dispersions, even if they do not give a direct measure of the catalytically relevant surface fraction of silver accessible, i.e., of real, intrinsic activities. In Table 2 we add for comparison the corresponding activities per gram of silver.

**3.2. Catalytic Hydrogenation of Crotonaldehyde over $Ag/SiO_2$ Catalysts.** The hydrogenation of crotonaldehyde over these silica-supported silver catalysts gave crotyl alcohol as a main product (see last column of Table 2) as a consequence of the preferred hydrogenation of the C=O group. The competitive reaction to *n*-butyraldehyde mainly accounts for the difference to 100%, whereas the rate of formation of *n*-butanol by consecutive hydrogenation remains always low under the reaction conditions applied. Table 2 shows that the selectivity to the unsaturated alcohol is independent of the Ag particle size in the range of 3.7 nm $\leq \bar{d}_{Ag} \leq$ 6.3 nm. The average value of crotyl alcohol selectivity is (59 $\pm$ 3)%. In comparing the turnover frequencies for silica-supported Ag particles in the size range 3.7−6.3 nm, also the TOF's of the five catalysts are similar in magnitude, yielding a mean value of $(1.0 \pm 0.5) \times 10^{-3}$ $s^{-1}$. For the activity per gram of silver, a mean value of $(6.3 \pm 3.0)$ $\mu$mol $g_{Ag}^{-1}$ $s^{-1}$ can be calculated from the data of

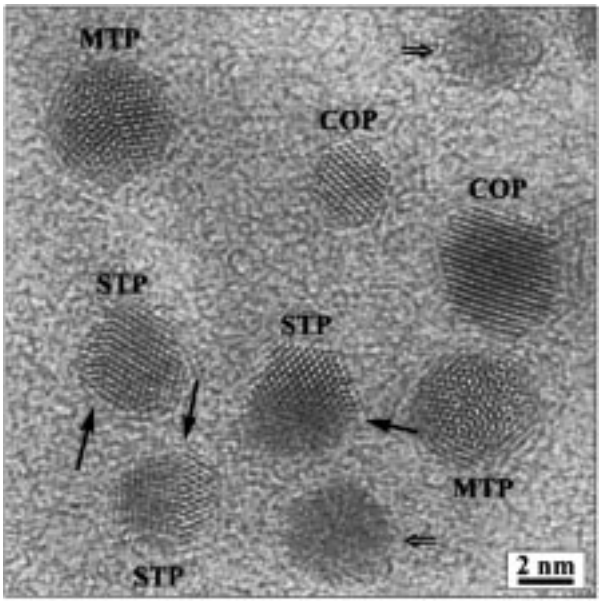


**Figure 3.** HRTEM image of Ag particles of various shape and composition (catalyst $Ag/SiO_2$-SG 1). Single-crystalline particles of cuboctahedral shape are designated by COP. STP denotes particles with a single twin boundary (indicated by a solid arrow) and MTP labels multiply twinned particles. Open arrows point to particles out of Bragg orientation that do not show lattice plane contrasts.

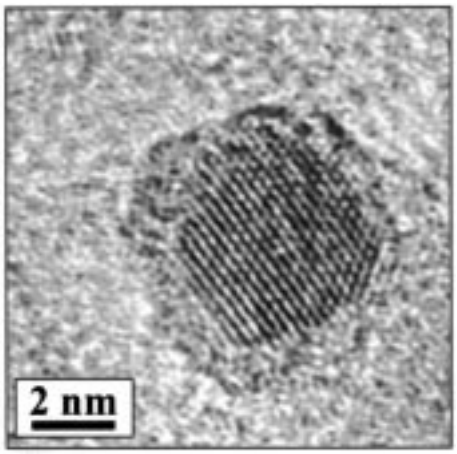


**Figure 4.** Cuboctahedral Ag particle of catalyst $Ag/SiO_2$-SG 3 covered by an amorphous shell.

Table 2. From these relatively small variations, which exhibit no clear trend with particle size, and from the observation of constant selectivity it can be concluded that the hydrogenation of crotonaldehyde, over the $Ag/SiO_2$ catalysts used, appears to be structure-insensitive. However, a particular catalytic system can exhibit structure sensitivity in only a small range of the particle sizes.[74−76] Therefore, the above conclusion requires testing with catalysts of appropriately large dispersion up to almost 100%, i.e., with ultradispersed Ag particles ($\bar{d}_{Ag} \ll 3$ nm).

**3.3. Nanostructural Characterization of $Ag/TiO_2$ Catalysts.** Our titania-supported 7 wt % silver catalyst prepared by the incipient wetness technique, using an aqueous solution of $AgNO_3$ and $TiO_2$ as decribed in the experimental part, fulfilled the above-mentioned requirement on the dispersion range. The $Ag/TiO_2$ sample was calcined in flowing air at 673 K, and after low-temperature (473 K, LTR) or high-temperature (773 K, HTR) reduction in flowing hydrogen significant changes in color, silver particle size, and catalytic properties were observed. The initial (dried) sample was of white color, which changes to black after calcination. The following LTR step gave gray samples, whereas the calcined catalyst treated with hydrogen under HTR conditions underwent a color change to dark blue. The LTR and HTR treatments did not give a change in the catalyst texture, since identical data for the BET surface area (35 $m^2\ g^{-1}$), pore volume (0.24 $cm^3\ g^{-1}$), and pore diameter (24 nm) were obtained for both the $Ag/TiO_2$-LTR and $Ag/TiO_2$-HTR catalyst. In addition, changes of the phase composition of titania were not observed by X-ray measurements, implying a phase transformation from anatase to rutile did not occur during the high-temperature treatment of the titania-supported silver catalyst.

Figure 5 shows CTEM overviews, HRTEM detail views, and the size distribution of the catalyst $Ag/TiO_2$-LTR (a) and catalyst $Ag/TiO_2$-HTR (b). Different from the $Ag/SiO_2$ catalysts, the support material is of crystalline nature. Since the support grains, randomly oriented with respect to the carbon film, show only faint contrast if not in Bragg orientation, metal particles sitting on their surface may be imaged unambiguously even by CTEM. Compared to silica-supported catalysts, the Ag particles exhibit a rather narrow size distribution and very low mean particle size ($\bar{d}_{Ag} = 2.8 \pm 1.9$ nm for $Ag/TiO_2$-LTR, $\bar{d}_{Ag} = 1.4 \pm 0.5$ nm for $Ag/TiO_2$-HTR), i.e., an exceedingly high dispersion that is mostly pronounced for the HTR catalyst. The corresponding values for the silver dispersion calculated from the mean particle size amount to 0.46 and 0.69. Thus, the reduction temperature had a marked influence on the silver particle size, which is decreased with increasing reduction temperature yielding ultradispersed particles after reduction at 773 K. To the best of our knowledge, the HTR catalyst with 1.4 nm sized silver particles prepared in the present study is the most highly dispersed silver catalyst yet reported. In addition, it can be concluded that sintering of silver did not occur during the high-temperature treatment.

The titania grains tend to stick to each other to form larger aggregates. This allows imaging of Ag particles in profile view without the underlying amorphous carbon contrast at places where chains and tangles of titania grains are bridging holes in the carbon film. As may be recognized from HRTEM images, Ag particles on titania do not exhibit a completely spherical shape but rather that of spheres truncated at the distinctly flat Ag/titania interface. This points to a metal−support interaction increased in comparison to the silica-supported catalysts. Even for the extremly small sizes present here, the Ag particles may be classified into monocrystalline, single-twinned, and multiply twinned structures, respectively, as observed for Ag on silica. Although there are no "support-free" particles found at the titania-supported catalysts, the crystalline nature of the support material enables detection of very thin amorphous layers covering the titania grains as well as part of the metal particles. In Figure 6 this is shown for both titania-supported catalysts. The metal particles being in close contact with the titania support are partly covered at the $Ag/TiO_2$-LTR catalyst and occasionally completely embedded at the $Ag/TiO_2$-HTR catalyst by amorphous layers. From a comparison and rating of more extended regions, it follows that the amorphous layers, the nature of which yet must remain unclear, are more closed and markedly thicker at the $Ag/TiO_2$-HTR catalyst.

**3.4. Particle Size Effects in the Catalytic Hydrogenation of Crotonaldehyde over $Ag/TiO_2$ Catalysts.** Again, to evaluate the catalytic properties, gas-phase hydrogenation of crotonaldehyde was carried out. The most important result from these experiments obtained with ultradispersed $Ag/TiO_2$, namely, a strong dependence of selectivity from the silver particle size in

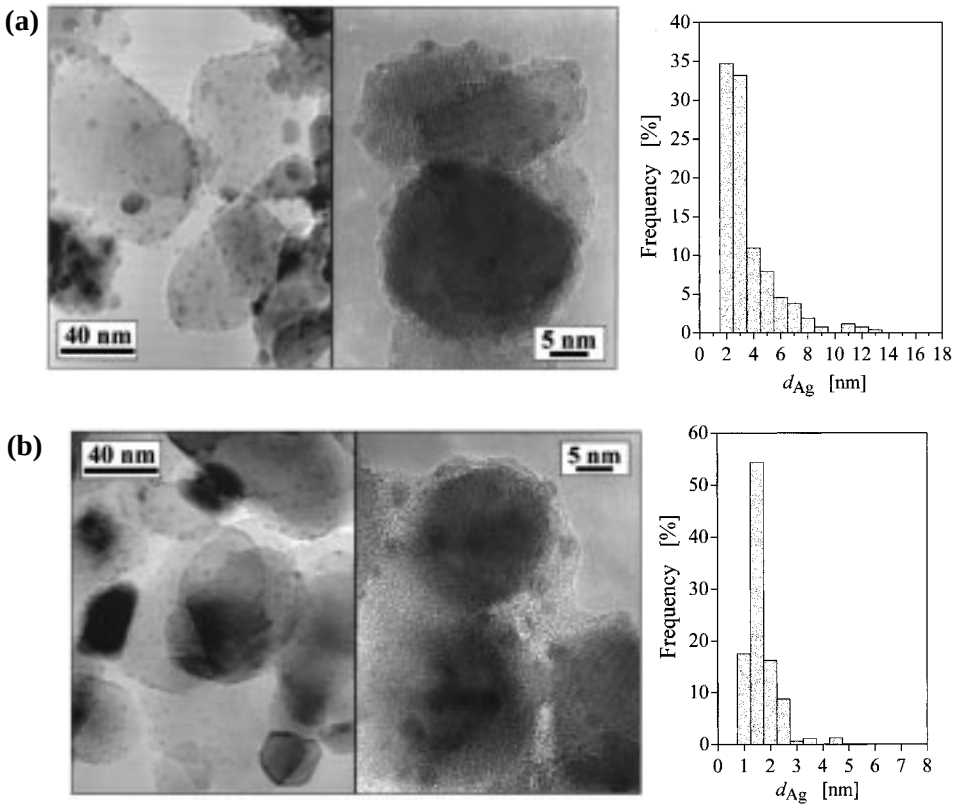


**Figure 5.** CTEM overview (left), HRTEM detailed view (center), and size distribution (right) of the catalyst Ag/$TiO_2$-LTR (a) and of catalyst Ag/$TiO_2$-HTR (b).

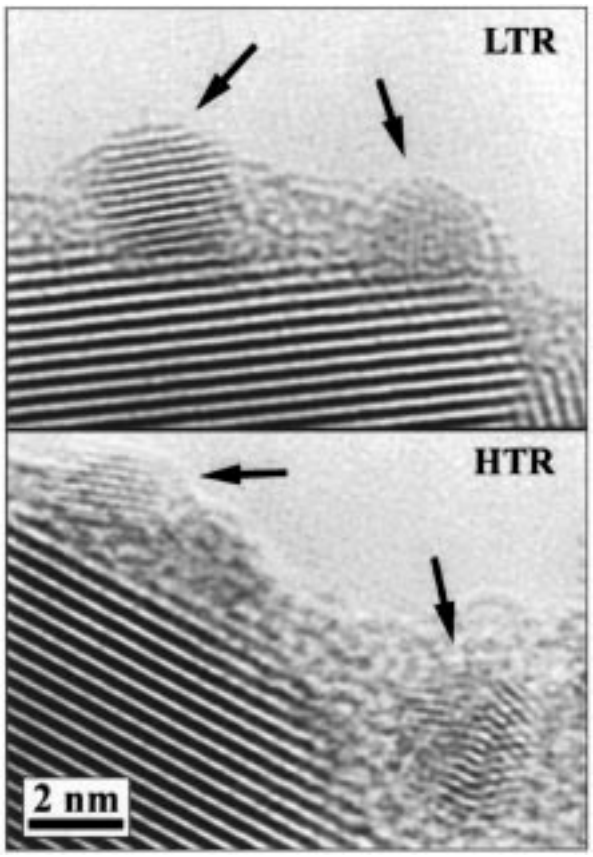


**Figure 6.** Amorphous layers covering titania grains and part of the metal particles (indicated by arrows) of catalyst Ag/$TiO_2$-LTR (top) and of catalyst Ag/$TiO_2$-HTR (bottom).

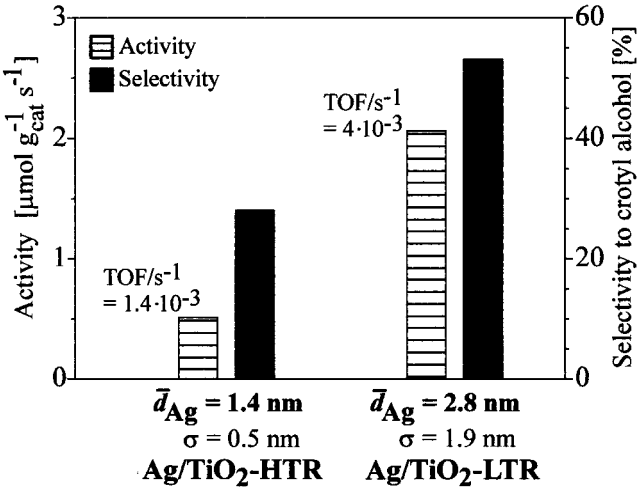


**Figure 7.** Activity (expressed as $\mu$mol $g_{cat}^{-1}$ $s^{-1}$ and turnover-frequency TOF) and selectivity toward crotyl alcohol in the gas-phase hydrogenation of crotonaldehyde over the catalysts Ag/$TiO_2$-LTR and Ag/$TiO_2$-HTR exhibiting a silver particle size of 2.8 and 1.4 nm, respectively (reaction conditions: $T$ = 453 K, $p_{total}$ = 2 MPa, molar ratio $H_2$/crotonaldehyde = 20).

the range $1.4 \leq \bar{d}_{Ag} \leq 2.8$ nm, can be seen in Figure 7. The selectivity to the unsaturated alcohol increases with increasing silver particle size; i.e., the 2.8 nm Ag particles on the low-temperature reduced catalyst gave a higher selectivity to crotyl alcohol (53%) than the ultradispersed 1.4 nm Ag particles of the high-temperature-reduced catalyst that produced crotyl alcohol with a selectivity of only 28%. In addition to this marked shift in selectivity to the unsaturated alcohol with increasing silver particle size, an enhancement of both the specific activity (per gram of silver) and the turnover-frequency on the Ag/$TiO_2$-LTR catalyst was observed compared with the HTR catalyst having the smaller silver particles. These results show that the hydrogenation of crotonaldehyde over these Ag catalysts can

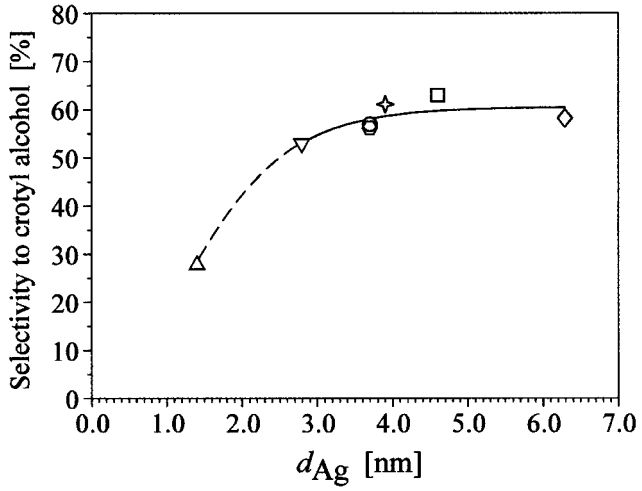


**Figure 8.** Selectivity toward crotyl alcohol depending on the silver particle size. (- - -) Titania-supported silver catalysts: (△) $Ag/TiO_2$-HTR, (▽) $Ag/TiO_2$-LTR; (—) silica-supported silver catalysts: (⬠) $Ag/SiO_2$-SG1, (○) $Ag/SiO_2$-SG3, (open star) $Ag/SiO_2$-I, (□) $Ag/SiO_2$-SG2, (◇) $Ag/SiO_2$-P).

be classified as structure-sensitive, indicating that the rate-determining step depends critically on the silver particle size and thus on the silver surface structure. Note that this structure sensitivity, which is of antipathetic character, appeared only for silver particles with sizes less than 3 nm, i.e., in a catalytic system that is conventionally designated to be of limited structure sensitivity.[74] Thus, the existence of structure sensitivity illustrates the importance of preparing small supported silver particles with sizes around the critical value of about 2 nm. Systems of limited structure sensitivity should be structure-insensitive for particle sizes greater than 5 nm,[74] and as shown in Figure 8, this seems to hold for the hydrogenation of crotonaldehyde over the silver catalysts of the present study. The marked increase of the selectivity to the desired product, crotyl alcohol, from 28% to 53% was observed in the range of silver particle size between 1.4 and 2.8 nm, whereas the selectivity remained nearly unchanged (56−63%) at particle sizes higher than 3 nm.

Note that the construction of Figure 8, which shows the dependence of selectivity on silver particle size for all silica- and titania-supported silver catalysts needs further explanation. First, to determine the catalyst activity (turnover-frequency) under differential conditions (i.e., at conversions lower than 20%), it was necessary to carry out the hydrogenation of crotonaldehyde over $Ag/SiO_2$ and $Ag/TiO_2$ at 413 and 453 K, respectively. However, the selectivities to the primary products, crotyl alcohol and *n*-butyraldehyde, did not depend on the temperature; it is an advantage of the use of silver catalysts that they do not catalyze secondary reactions (further hydrogenation to the saturated alcohol, formation of hydrocarbons) to a greater extent at temperatures up to 493 K.[4,46] Thus, data points of the crotyl alcohol selectivity, measured at two different temperatures, can be included in a common figure. Second, it should be excluded that recording the effect of the particle size on catalytic behavior is influenced by metal−support interactions, even in the case of $TiO_2$. It is well-known that for platinum group metals supported on $TiO_2$ a large decrease of $H_2$ and CO chemisorption capacity after a high-temperature reduction occurs, attributed to a strong metal support interaction (SMSI).[77−79] However, since silver does not chemisorb carbon monoxide and hydrogen to an appreciable extent unless in the presence of strongly bound oxygen,[73,80−83] $O_2$ chemisorption was conducted on the LTR and HTR titania-supported Ag

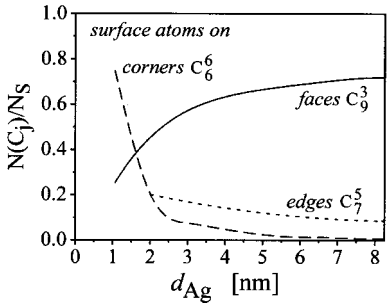


**Figure 9.** Relative occurrence $N(C_j)/N_s$ of various types of surface atoms $C_j$ as a function of the silver particle size $d_{Ag}$ (according to van Hardeveld and Hartog[84]): $C_6^6$, corner atom sites; $C_7^5$, edge atom sites between cube and octahedron faces; $C_9^3$, face atoms on close-packed octahedron faces.

samples of the present study. Whereas oxygen chemisorption of the $Ag/TiO_2$-LTR catalyst gave an apparent dispersion (O/Ag, fraction exposed) of 0.78 assuming an $O_{ad}/Ag_s$ ratio of unity, a 30% decrease (O/Ag = 0.56) was estimated for the $Ag/TiO_2$-HTR catalyst. However, we recall that the size distributions obtained from HRTEM micrographs (see Figure 5) unequivocally show a significantly smaller silver particle size, i.e., higher silver dispersion for the $Ag/TiO_2$-HTR catalyst. As shown above, inspection of HRTEM images revealed that the apparent inconsistency between dispersion data deduced from chemisorption and electron microscopy is clearly a result of an amorphous thin layer covering the silver crystallites without changes in their morphology. Note that the chemisorption itself can be structure-sensitive caused by changes in particle shape, in the proportion of exposed planes, or in the roughness of the metal surface.[74−76]

To explain the silver particle size effect on the intramolecular selectivity, the surface structure of metallic particles, as characterized at first approximation by the coordination number of surface atoms, shall be considered in the size range of 1−5 nm. The arrangement of surface atoms (on faces, edges, and corners) in small particles was described by calculations of van Hardeveld and Hartog.[84] According to this work, Figure 9 shows the fraction of surface atoms of various coordination depending on the size of a silver particle of cuboctahedral shape. Apparently, the fraction of face atoms, i.e., of low-index planes, increases with increasing particle size, whereas the fraction of metal atoms on edges and corners, i.e., of highly exposed atoms, decreases. If hydrogenation of the C=O group of the α,β-unsaturated aldehyde is favored by face atoms, the increasing fraction of Ag(111) planes of larger silver particles would give higher rates of the formation of the unsaturated alcohol and, thus, in selectivity. This corresponds to antiphatetic structure sensitivity[74] and is, as indicated by comparing the size dependence of selectivity (Figure 8) and relative occurrence of $\bar{d}_{Ag}$ face atoms (Figure 9), exactly the result that we observed in crotonaldehyde hydrogenation over the silver catalysts of the present study. The importance of the crystallographic orientation of metal surfaces for the selectivity in the hydrogenation of α,β-unsaturated aldehydes was clearly demonstrated by Delbecq and Sautet studying adsorption modes on well-defined surfaces by means of semiemperical extended Hückel calculations.[57] Generally, dense (111) crystal faces were concluded to be not very favorable for coordination of the C=C group and, thus, the increase of the fraction of this face with increasing particle size compared to the fraction of highly exposed metal atoms should improve the selectivity toward the unsaturated alcohol. These theoretical results agree with the experimental studies on different well-defined single-crystal platinum surfaces.[58−60] On

silver surfaces, bifunctional intermediates such as 2-alkenyloxy could operate as precursors of unsaturated alcohols[46] and were observed indeed on silver surfaces using NEXAFS, TPRS, and HREELS−TPD measurements.[85−87] However, experimental and theoretical studies on the preferred adsorption mode of α,β-unsaturated aldehydes on silver surfaces are not available.

Concerning the role of silver in an SMSI interaction, Baker et al. reported, by using TEM, that the reduction of Ag on titania at temperatures (823 K) higher than those employed in the present study results in quite normal behavior of the metal, the silver particles were large, relatively dense, and globular in outline.[88] Electron diffraction examination indicated that reduction of titania did not occur. The effect of different reducing pretreatments on a highly dispersed titania-supported silver catalyst was studied by Gonzalez-Elipe et al. using EPR spectroscopy.[89] The formation of silver aggregates produced by reduction treatment in hydrogen at 473 K was explained to proceed through an electron transfer from the $TiO_2$ surface to $Ag^+$ species. The observed $Ti^{3+}$ signal was always much smaller on $Ag/TiO_2$ than that obtained on $TiO_2$ without silver treated in hydrogen under similar conditions, which indicates a partial reduction of the support. The conclusion of some kind of metal−support interaction drawn by the authors is, however, debatable because EPR measurements are very sensitive, detecting $Ti^{3+}$ ions already at a small extent of reduction. Note that even in the case of typical metal catalysts (e.g., Pt) in the SMSI state, values between 0.04% and 1% for the $Ti^{3+}/Ti^{4+}$ ratio were determined by EPR.[36]

Since real catalysts exhibit a distribution of metal particle sizes, it seems plausible that the interpretation of particle size effects by pure geometric reasons may be more complicated than that described by mathematical models based on regular small crystallites.[84] Changes in the surface atom coordination are, of course, linked to changes in electronic effects that cannot be absolutely ruled out. Therefore, we are conducting EPR and XPS measurements[90] to examine whether the antipathetic structure sensitivity in the range of silver particle sizes of about 1−2 nm, i.e., for clusters of $n < 150$, can be attributed to unusual electronic properties of nanosized silver.

## 4. Conclusions

The results reported in the present paper showed the important impact of conventional and high-resolution electron microscopy on the examination of particle size effects in the gas-phase hydrogenation of α,β-unsaturated aldehydes over silver-based catalyst. In the hydrogenation of crotonaldehyde high selectivity toward the desired unsaturated alcohol (product of C═O group hydrogenation) was obtained on catalysts containing mainly silver particles with dense Ag(111) surface planes, whereas the dominating high-index planes (low-coordinated atoms) in smaller-sized silver particles gave lower selectivity. Although the application of silver catalysts for selective hydrogenation of bifunctional organic compounds containing C═O functional groups remains rather unusual, the observed catalytic behavior agrees well with hydrogenation studies over supported platinum catalysts and confirms that the selectivity can be controlled by the particle size influencing the adsorption mode of the α,β-unsaturated aldehyde. Moreover, application of the sol−gel technique and impregnation as preparation methods followed by appropriate methods of pretreatment allows us to obtain well-dispersed silver catalysts. The interpretation of antipathetic structure sensitivity for silver particles smaller than 3 nm in size requires further confirmation by studying catalysts with broader variation of particle sizes to clarify the role of additional electronic effects.

**Acknowledgment.** This work has been supported by the Bundesminister für Bildung, Wissenschaft, Forschung und Technologie (BMBF, Project-No. 03D0028A0). Assistance by M. Lucas in experimental work has been greatly appreciated. The authors thank KataLeuna GmbH Catalysts for conducting chemisorption measurements.

## References and Notes

(1) Rylander, P. N. *Catalytic Hydrogenation in Organic Syntheses*; Academic Press: New York, 1979; p 74.

(2) Sokol'skii, D. V.; Anisimova, N. V.; Zharmagambetova, A. K.; Mukhamedzhanova, S. G.; Edygenova, L. N. *React. Kinet. Catal. Lett.* **1987**, *33*, 399.

(3) Claus, P.; Hönicke, D. In *Catalysis of Organic Reactions*; Chemical Industries Series 62; Scaros, M. G., Prunier, M. L., Eds.; Marcel Dekker: New York, 1995; p 431.

(4) Claus, P.; Kraak, P.; Schödel, R. Heterogeneous Catalysis and Fine Chemicals IV. In *Studies in Surface Science and Catalysis*; Blaser, H. U., Baiker, A., Prins, R., Eds.; Elsevier: Amsterdam, 1997; Vol. 108, p 281.

(5) Raab, C. G.; Englisch, M.; Marinelli, T. B. L. W.; Lercher, J. A. Heterogeneous Catalysis and Fine Chemicals III. In *Studies in Surface Science and Catalysis*; Guisnet, M., Barbier, J., Barrault, J., Bouchoule, C., Duprez, D., Pérot, G., Montassier, C., Eds.; Elsevier: Amsterdam, 1993; Vol. 78, p 211.

(6) Raab, C. G.; Lercher, J. A. *J. Mol. Catal.* **1992**, *75*, 71.

(7) Marinelli, T. B. L. W.; Naaburs, S.; Ponec, V. *J. Catal.* **1995**, *151*, 431.

(8) Waghray, A.; Wang, J.; Oukaci, R.; Blackmond, D. G. *J. Phys. Chem.* **1992**, *96*, 5954.

(9) Waghray, A.; Blackmond, D. G. *J. Phys. Chem.* **1993**, *97*, 6002.

(10) Marinelli, T. B. L. W.; Vleeming, J. H.; Ponec, V. New Frontiers in Catalysis. In *Studies in Surface Science and Catalysis*; Guczi, L., Solomosi, F., Tétényi, P., Eds.; Elsevier: Amsterdam, 1993; Vol. 75, p 1211.

(11) Goupil, D.; Foullioux, P.; Maurel, R. *React. Kinet. Catal. Lett.* **1987**, *35*, 185.

(12) Coq, B.; Figueras, F.; Moreau, C.; Moreau, P.; Warawdekar, M. *Catal. Lett.* **1993**, *22* 189.

(13) Patil, A. N.; Banares, M. A.; Lei, X.; Fehlner, T. P.; Wolf, E. E. *J. Catal.* **1996**, *159*, 458.

(14) Rylander, P. N. *Catalytic Hydrogenation over Platinum Metals*; Academic Press: New York, 1967; p 249.

(15) Richard, D.; Ockelford, J.; Girior-Fendler, A.; Gallezot, P. *Catal. Lett.* **1989**, *3*, 53.

(16) Galvagno, S.; Donato, A.; Neri, G.; Pietropaolo, R.; Pietropaolo, D. *J. Mol. Catal.* **1989**, *49*, 223.

(17) Galvagno, S.; Donato, A.; Neri, G.; Pietropaolo, R. *Catal. Lett.* **1991**, *8*, 9.

(18) Poltarzewski, Z.; Galvagno, S.; Pietropaolo, R.; Staiti, P. *J. Catal.* **1986**, *102*, 190.

(19) Tronconi, E.; Crisafulli, C.; Galvagno, S.; Donato, A.; Neri, G.; Pietropaolo, R. *Ind. Eng. Chem. Res.* **1990**, *29*, 1766.

(20) Blackmond, D. G.; Oukazi, R.; Blanc, B.; Gallezot, P. *J. Catal.* **1991**, *131*, 401.

(21) Blackmond, D. G.; Waghray, A.; Oukaci, R.; Blanc, B.; Gallezot, P. Heterogeneous Catalysis and Fine Chemicals II. In *Studies in Surface Science and Catalysis*; Guisnet, M., Barrault, J., Bouchoule, C., Duprez, D., Pérot, G., Maurel, R., Montassier, C., Eds.; Elsevier: Amsterdam, 1991; Vol. 59, p 145.

(22) Richard, D.; Fouilloux, P.; Gallezot, P. Characterization and Metal Catalysts. In *Proceedings of the 9th International Congress on Catalysis*; Phillips, M. J., Ternan, M., Eds.; Calgary, 1988; p 1074.

(23) Giroir-Fendler, A.; Richard, D.; Gallezot, P. Heterogeneous Catalysis and Fine Chemicals. In *Studies in Surface Science and Catalysis*; Guisnet, M., Barrault, J., Bouchoule, C., Duprez, D., Montassier, C., Pérot, G., Eds.; Elsevier: Amsterdam, 1988; Vol. 41, p 171.

(24) Gallezot, P.; Giroir-Fendler, A.; Richard, D. *Catal. Lett.* **1990**, *5*, 169.

(25) Gallezot, P.; Blanc, B.; Barthomeuf, D.; Pais da Silva, M. I. Zeolites and Related Microporous Materials: State of the Art 1994. In *Studies in Surface Science and Catalysis*; Weitkamp, J., Karge, H. G., Pfeifer, H. Hölderich, W., Eds.; Elsevier: Amsterdam, 1994; Vol. 84, p 1433.

(26) Didillon, B.; El Mansour, A.; Candy, J. P.; Bournonville, J. P.; Basett, J.-M. Heterogeneous Catalysis and Fine Chemicals II. In *Studies in Surface Science and Catalysis*; Guisnet, M., Barrault, J., Bouchoule, C., Duprez, D., Pérot, G., Maurel, R., Montassier, C., Eds.; Elsevier: Amsterdam, 1991; Vol. 59, p 137.

(27) Didillon, B.; Candy, J. P.; Le Peletier, F.; Ferretti, O. A.; Basett, J.-M. Heterogeneous Catalysis and Fine Chemicals III. In *Studies in Surface Science and Catalysis*; Guisnet, M., Barbier, J., Barrault, J., Bouchoule,

C., Duprez, D., Pérot, G., Montassier, C., Eds.; Elsevier: Amsterdam, 1993; Vol. 78, p 147.
(28) Candy, J. P.; Didillon, B.; Smith, E. L.; Shay, T. B.; Basset, J.-M. *J. Mol. Catal.* **1994,** *86*, 179.
(29) Vannice, M. A.; Sen, B. *J. Catal.* **1989**, *115*, 65.
(30) Yoshitake, H.; Asahma, K.; Iwasawa, Y. *J. Chem. Soc., Faraday Trans. 1* **1989**, *85*, 2021.
(31) Yoshitake, H.; Iwasawa, Y. *J. Catal.* **1990**, *125*, 227.
(32) Claus, P.; Selent, D. *Chem.-Ing.-Tech.* **1995**, *67*, 586.
(33) Raab, C. G.; Lercher, J. A. *Catal. Lett.* **1993**, *18*, 99.
(34) Kasper, J.; Graziani, M.; Picasso Escobar, G.; Trovarelli, A. *J. Mol. Catal.* **1992**, *72*, 243.
(35) Coq, B.; Kumbhar, P. S.; Moreau, C.; Moreau, P.; Figueras, F. *J. Phys. Chem.* **1994**, *98*, 10180.
(36) Claus, P.; Schimpf, S.; Schödel, R.; Kraak, P.; Mörke, W. Hönicke, D. *Appl. Catal.* **1997**, *165*, 429.
(37) Englisch, M.; Jentys, A.; Lercher, J. A. *J. Catal.* **1997**, *166*, 25.
(38) Hutchings, G. J.; King, F.; Okoye, I. P.; Rochester, C. H. *Appl. Catal.* **1992**, *83*, L7.
(39) Marinelli, T. B. W. L.; Ponec, V. *J. Catal.* **1995**, *156*, 51.
(40) Hutchings, G. J.; King, F.; Okoye, I. P.; Bradley, M. B.; Rochester, C. H. *J. Catal.* **1994**, *148*, 453.
(41) Claus, P. In *Catalysis of Organic Reactions;* Malz, R. E., Ed.; Chemical Industries Series 68; Marcel Dekker: New York, 1996; p 419.
(42) Bakhanova, E. N.; Astakhova, A. S.; Brikenshtein, Kh. A.; Dorokhov, V. G.; Savchenko, V. I.; Khidekel, M. L. *Izs. Akad. Nauk SSSR, Ser. Khim.* **1972**, *9*, 1993.
(43) Sokol'skii, D. V.; Zharmagambetova, A. K.; Anisova, N. V.; Ualikhanova, A. *Dokl. Akad. Nauk SSSR* **1983**, *273*, 151.
(44) Neri, G.; Mercadante, L.; Donato, A.; Visco, A. M.; Galvagno, S. *Catal. Lett.* **1994**, *29*, 379.
(45) Nitta, Y.; Kato, T.; Imanaka, T. Heterogeneous Catalysis and Fine Chemicals III. In *Studies in Surface Science and Catalysis*; Guisnet, M., Barbier, J., Barrault, J., Bouchoule, C., Duprez, D., Pérot, G., Montassier, C., Eds.; Elsevier: Amsterdam, 1993; Vol. 78, p 83.
(46) Claus, P. Part II "Fine Chemicals Catalysis". In *Topics in Catalysis*; Somorjai, G. A., Thomas, J. M., Blackmond, D., Leitner, W., Eds.; Baltzer Science Publishers BV: Bussum, The Netherlands, 1998; Vol. 5, p 51.
(47) Nitta, Y.; Hiramatsu, Y.; Imanaka, T. *Chem. Express* **1989**, *4*, 281.
(48) Nitta, Y.; Ueno, K.; Imanaka, T. *Appl. Catal.* **1989**, *56*, 9.
(49) Nitta, Y.; Hiramatsu, Y.; Imanaka, T. *J. Catal.* **1990**, *126*, 235.
(50) Giroir-Fendler, A.; Gallezot, P.; Richard, D. *Catal. Lett.* **1990**, *5*, 175.
(51) Galvagno, S.; Capannelli, G.; Neri, G.; Donato, A.; Pietropaolo, R. *J. Mol. Catal.* **1991**, *64*, 237.
(52) Minot, C.; Gallezot, P. *J. Catal.* **1990**, *123*, 341.
(53) Galvagno, S.; Milone, C.; Donato, A.; Neri, G.; Pietropaolo, R. *Catal. Lett.* **1993**, *18*, 349.
(54) Galvagno, S.; Milone, C.; Neri, G.; Donato, A.; Pietropaolo, R. Heterogeneous Catalysis and Fine Chemicals III. In *Studies in Surface Science and Catalysis*; Guisnet, M., Barbier, J., Barrault, J., Bouchoule, C., Duprez, D., Pérot, G., Montassier, C., Eds.; Elsevier: Amsterdam, 1993; Vol. 78, p 163.
(55) Coq, B.; Figueras, F.; Geneste, P.; Moreau, C.; Moreau, P.; Warawdekar, M. *J. Mol. Catal.* **1993**, *78*, 211.
(56) Englisch, M.; Jentys, A.; Lercher, J. A. *J. Catal.* **1997**, *166*, 25.
(57) Delbecq, F.; Sautet, P. *J. Catal.* **1995**, *152*, 217.
(58) Berthier, Y.; Pradier, C.-M. *Bull. Soc. Chim. Fr.* **1997**, *134*, 773.
(59) Birchem, T.; Pradier, C. M.; Berthier, Y.; Cordier, G. *J. Catal.* **1994**, *146*, 503.
(60) Pradier, C. M.; Birchem, T.; Berthier, Y.; Cordier, G. *Catal. Lett.* **1994**, *29*, 371.
(61) Birchem, T.; Pradier, C. M.; Berthier, Y.; Cordier, G. *J. Catal.* **1996**, *161*, 68.
(62) Berndt, H.; Mehner, H.; Claus, P. *Chem.-Ing.-Tech.* **1995**, *67*, 1332.
(63) Rupprechter, G.; Hayek, K.; Hofmeister, H. *J. Catal.* **1998**, *173*, 409.
(64) Bernal, S.; Calvino, J. J.; Gatica, J. M.; Larese, C.; López-Cartes, C.; Pérez-Omil, J. A. *J. Catal.* **1997**, *169*, 510.
(65) Rasband, W. *NIH Image* (public domain software); U.S. National Institute of Health. FTP: zippy.nimh.nih.gov.
(66) Schödel, R.; Keck, M.; Neubauer, H.-D. *Chem. Technol.* **1992**, *44*, 93.
(67) Lucas, M.; Claus, P. *Chem.-Ing.-Tech.* **1995**, *67*, 773.
(68) Hofmeister, H. *Cryst. Res. Technol.* **1998**, *33*, 3.
(69) Koeppel, R. A.; Baiker, A.; Wokaun, A. *Appl. Catal.* **1992**, *84*, 77.
(70) Razi Seyedmonir, S.; Plischke, J. K.; Strohmeyer, D. E.; Vannice, M. A.; Young, H. W. *J. Catal.* **1990**, *123*, 534.
(71) Azomoza, M.; Lopez, T.; Gomez, R.; Gonzalez, R. D. *Catal. Today* **1992**, *15*, 547.
(72) Strubinger, L. M.; Geoffroy, G. L.; Vannice, M. A. *J. Catal.* **1985**, *96*, 72.
(73) Plischke, J. K.; Vannice, M. A. *Appl. Catal.* **1988**, *42*, 255.
(74) Che, M.; Bennett, C. O. *Adv. Catal.* **1989**, *36*, 55.
(75) Bond, G. *Acc. Chem. Res.* **1993**, *26*, 490.
(76) Bond, G. *Chem. Soc. Rev.* **1991**, *20*, 441.
(77) Tauster; S. J.; Fung, S. C.; Garden, R. L. *J. Am. Chem. Soc.* **1978**, *100*, 170.
(78) Haller, G. L.; Resasco, D. E. *Adv. Catal.* **1989**, *36*, 173.
(79) Lamber, R.; Jaeger, N.; Schulz-Ekloff, G. *Chem.-Ing.-Tech.* **1991**, *63*, 681.
(80) Razi Seyedmonir, S.; Strohmeyer, D. E.; Geoffroy, G. L.; Vannice, M. A.; Young, H. W.; Linowski, J. W. *J. Catal.* **1984**, *87*, 424.
(81) Razi Seyedmonir, S.; Strohmeyer, D. E.; Guskey, G. J.; Geoffroy, G. L.; Vannice, M. A. *J. Catal.* **1985**, *93*, 288.
(82) Scholten, J. J. F.; Konvalinka, J. A.; Beekman, F. W. *J. Catal.* **1973**, *28*, 209.
(83) Sandler, Y. L.; Beer, S. Z.; Durigon, D. D. *J. Phys. Chem.* **1966**, *70*, 3881.
(84) Van Hardeveld, R.; Hartog, F. *Surf. Sci.* **1969**, *15*, 189.
(85) Solomon, J. L.; Madix, R. J. *J. Phys. Chem.* **1987**, *91*, 6241.
(86) Solomon, J. L.; Madix, R. J.; Stöhr, J. *J. Chem. Phys.* **1988**, *89*, 5316.
(87) Carter, R.; Brad Anton, A.; Apai, G. *Surf. Sci.* **1993**, *290*, 319.
(88) Baker, R. T.; Prestridge, E. B.; Murrell, L. L. *J. Catal.* **1983**, *79*, 348.
(89) Gonzales-Elipe, A. R.; Soria, J.; Munuera, G. *J. Catal.* **1982**, *76*, 254.
(90) Brückner, A.; Grünert, W.; Hofmeister, H.; Claus, P. To be submitted.